Environ Fluid Mech (2010) 10:103–120
DOI 10.1007/s10652-009-9147-2

ORIGINAL ARTICLE

Quantification of advective solute travel times and mass transport through hydrological catchments

Amélie Darracq · Georgia Destouni · Klas Persson · Carmen Prieto · Jerker Jarsjö

Received: 29 March 2009 / Accepted: 10 August 2009 / Published online: 25 August 2009

Abstract This study has investigated and outlined the possible quantification and mapping of the distributions of advective solute travel times through hydrological catchments. These distributions are essential for understanding how local water flow and solute transport and attenuation processes affect the catchment-scale transport of solute, for instance with regard to biogeochemical cycling, contamination persistence and water quality. The spatial and statistical distributions of advective travel times have been quantified based on reported hydrological flow and mass-transport modeling results for two coastal Swedish catchments. The results show that the combined travel time distributions for the groundwater-stream network continuum in these catchments depend largely on the groundwater system and model representation, in particular regarding the spatial variability of groundwater hydraulic parameters (conductivity, porosity and gradient), and the possible contributions of slower/deeper groundwater flow components. Model assumptions about the spatial variability of groundwater hydraulic properties can thus greatly affect model results of catchment-scale solute spreading. The importance of advective travel time variability for the total mass delivery of naturally attenuated solute (tracer, nutrient, pollutant) from a catchment to its downstream water recipient depends on the product of catchment-average physical travel time and attenuation rate.

Keywords Hydrology · Travel time · Solute transport · Natural attenuation · Catchment · Groundwater–surface water interactions

1 Introduction

Travel time distributions (or also called transit time distributions, system response functions, weighting functions [1]) are useful descriptors of how small-scale physical transport processes and their dynamics combine to determine larger-scale transport behavior in

A. Darracq (✉) · G. Destouni · K. Persson · C. Prieto · J. Jarsjö
Department of Physical Geography and Quaternary Geology, Stockholm University, Stockholm, Sweden
e-mail: amelie.darracq@natgeo.su.se

catchments. A travel time distribution can be determined from the mass flow response or breakthrough of an instantaneous, conservative tracer input in a catchment area with zero background tracer concentration [2]. This integrates the physical transport of tracer in all the pathways that carry it through the catchment into a single distribution of the timescales of the tracer transport through the catchment. This distribution quantifies the physical spreading of tracer mass in that catchment-scale transport process and can aid significantly in the understanding and quantification of the processes involved in the catchment-scale water flow and solute (tracer, nutrient, pollutant) transport [3–7]. These processes control also biogeochemical cycling, contamination persistence and water quality [8].

Purely physical, advective solute travel times through a catchment depend on the transport velocities and transport pathway lengths between the solute input and output locations. These physical transport quantities and associated solute travel times may vary widely for different solute input locations, an influence that may be referred to as geomorphologic dispersion in the stream networks [9] and analogously in the subsurface transport process from the land surface to the streams [3,5]. Even for solute input at a single well-defined point-source location in a stream, the downstream solute transport and travel times through the stream network are subject to dispersion due to transport velocity variations among and along different transport pathways [10,11]. The solute may also undergo diffusive mass transfer between mobile and immobile water in the hyporheic [12] and dead zones [13].

Different factors and mechanisms may control the dynamics and timescales of hydrological mass transport through drainage basins [14–17]. The travel time variability that exists at all scales in all catchments may to smaller or greater degree mask some important effects of these factors and mechanisms and lead to disparities between different solute transport models and results for different measurement and model scales [4,18–20]. Such disparities limit our capability to incorporate field knowledge and to interpret and transfer results in and between different modeling frameworks and catchments.

In general, realistic distributions of solute travel times in catchments have been pointed out as essential information for accurately representing the catchment-scale process of solute transport, yet commonly difficult to quantify and constrain [1]. In this paper, we investigate the possible quantification of solute travel time distributions in catchments, by the use of reported results on catchment-scale hydrological flow and mass transport modeling in two well-investigated, coastal Swedish catchments areas (Fig. 1): the Norrström drainage basin [19–24] and the Forsmark catchment area [25–28]. In particular, we investigate here the role of different possible groundwater system representations for the quantification of solute travel times through catchments. We further investigate the effects of different travel time distribution quantifications for the resulting solute mass transport from the catchments to downstream recipients.

2 Materials and methods

This section describes the general approach to quantify travel times and their spatial and statistical distributions in catchments, and the solute mass delivery from the catchments. The modeling details for the two specific investigated catchment areas are given in the Appendix.

2.1 General quantification approach

Numerous studies have in the past decades developed and used theoretical conceptualization and quantification approaches that account for the large-scale, physical spreading of solute

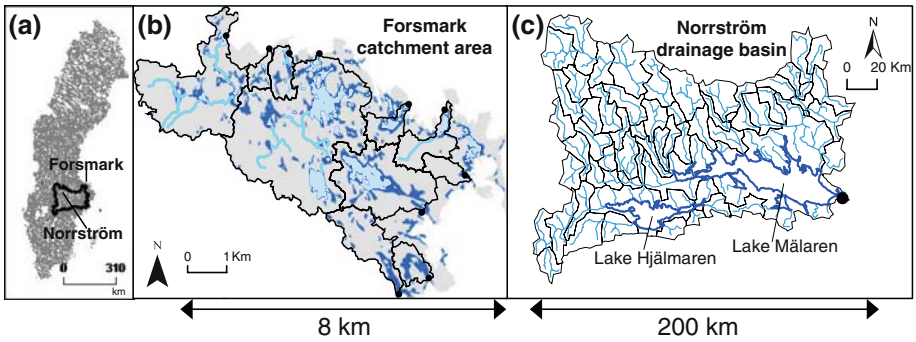

Fig. 1 **a** Location of the Forsmark and Norrström catchment areas within Sweden; **b** the Forsmark catchment area with its: surface water system, including streams (*blue lines*), lakes (*soft blue*), wetlands (*dark blue*) and ten main stream outlets to the coast (*black dots*), the subcatchment boundaries of which are drawn with black lines; and **c** the Norrström drainage basin with its: river network (*soft blue*), major lakes (*dark blue*) and subcatchment boundaries (*black lines*), and outlet to the sea (*black dot*). The small near-coastal zones in between the main stream outlets of the Forsmark catchment area discharge mainly groundwater to the sea

transport in heterogeneous geological formations in terms of prevailing advection variability; see for instance Dagan [29] and Rubin [30] for reviews of such different approaches. Some of these approaches have particularly developed the use of advective solute travel times and their distributions as a main basis for Lagrangian conceptualizations and derivations of field-scale solute transport and spreading in different subsurface water systems (unsaturated soil and groundwater, e.g. [2,31–47]). Parallel studies also extended the theoretical basis of the Lagrangian travel time-based approaches to link the solute transport through the different water subsystems (unsaturated soil, groundwater, streams and stream networks) that are hydraulically connected at the larger scales of hydrological catchments [4,5,44,48–50].

The advective travel time distributions that have been used in most previous studies have been approximated by assuming some common type of probability density function (e.g., log-normal, inverse Gaussian), which can be fully parameterized based on knowledge of only the possible mean and variance of solute travel times in the considered transport system. In this study, we adopt the Lagrangian advective travel time-based approach and extend it to quantify and investigate entire distributions of advective solute travel times in the two Swedish catchment cases and their different water subsystems, by the use of the flow and mass transport results that have already been modeled, tested against all available monitoring data and reported in a series of previous published studies of these catchment areas [19–28].

In general, studies that use Lagrangian advective travel time-based approaches do so because they focus on the macro-dispersion of solute transport due to large-scale advection variability. In such large-scale contexts, the local mixing that occurs between and along different advection pathways due to pore-scale dispersion and molecular diffusion in mobile water is often neglected [29,30]. However, if and where account of these processes is needed, they can be linked to the advective travel-time based model representations, with such linked studies showing that neglecting local dispersion and diffusion within mobile water does not much affect the large-scale mean mass flow rate or concentration, but may lead to the overestimation of local mass flux and concentration variances [51–54].

Jarsjö et al. [26] have also specifically investigated the effect of local random variability around mean advective travel time, e.g. due to local dispersion and diffusion, for the Forsmark catchment area, which constitutes one of the two specific catchment cases of the present

study. The results of Jarsjö et al. [26] confirm that also in this specific catchment case, the effect of such local variability within mobile water is small on the expected large-scale solute transport. The present paper therefore focuses on the quantification of advective solute travel times as the main, first and necessary step towards quantifying catchment-scale pollutant transport and its dominant timescales.

With regard to more significant effects of diffusive mass transfer between mobile and immobile water zones, it is one of the main advantages of Lagrangian travel time-based approaches that their first-step quantification of advective solute travel time distributions can readily be coupled with relevant process models of diffusive mass transfer [5,33,34, 36,37,46,49], as well as with biogeochemical reaction process models of various degrees of complexity [34,38–43,45,47,50,55]. The resulting coupled advection-sorption and/or advection-reaction models account then both for the physical solute spreading effect of advection variability and the diffusive mass transfer and/or biogeochemical reaction process effects on large-scale pollutant transport. In this study, this extension possibility will only be illustrated for a generic, hypothetical and simple case of solute undergoing first-order attenuation. This illustration is made to show some general first-order effects of the advective solute travel time variability and distributions on the large-scale solute mass delivery from different parts of a catchment area and the whole catchment to a downstream water recipient. More complex investigations of diffusive mass transfer and/or reactive transport of specific pollutants are outside the scope of the present study, but we note with reference to the above-cited diffusive-reactive transport studies that such investigations are facilitated by the present, first-step quantification of advective solute travel time distributions.

In the present quantification of these distributions, we further neglect the travel time components in the essentially vertical transport from the soil surface down to the groundwater table, for simplicity and in comparison to the dominant, large travel times in the groundwater system, from the groundwater table to the groundwater–stream interface. This is by no means any necessary neglect requirement in the Lagrangian advective travel time-based approach. On the contrary, this approach has already been developed and used for linking the travel times and travel time distributions of the essentially vertical unsaturated zone transport with the essentially horizontal transport in the groundwater zone and its travel times and travel time distributions, in order to represent the large-scale solute transport through the integrated soil–groundwater system [44,49]. If and where the advective travel times through the unsaturated zone are quantified or expected to be significant in relation to the groundwater travel times, the same methodology can readily be used to extend the present quantification results to consider and integrate the unsaturated zone travel time components in the combined catchment-scale travel time distribution.

Furthermore, the previously reported flow and transport modeling of the specific two Swedish catchment cases considered in this study certainly include soil properties and processes [19–28]. The main reason and motivation for the present primary focus on quantifying and linking the groundwater and stream network travel times is that the soil depth of quaternary deposits above the bedrock is generally small (around 1–2 m, up to maximum 5 m) in both these catchment areas, with the groundwater table being on average about one meter below the soil surface. In contrast, the horizontal transport lengths are three to five orders of magnitude greater in both the small Forsmark catchment area of 30 km^2 and the much larger Norrström catchment area of 22000 km^2 (Fig. 1). We believe that these conditions justify a primary focus on the advective travel times of the horizontal transport through the groundwater–surface water continuum, especially with the particular aim of the present study to investigate the role of different possible groundwater system characterizations and model representations for the quantification of solute travel times through catchments. Also in this

respect, the present results facilitate follow-up studies that can incorporate the additional travel time components of vertical transport through the unsaturated zone and investigate their effects on the combined total distributions of travel times through whole catchments.

2.2 General travel time and mass delivery fraction calculations

We consider solute mass releases from different sources on the land surface and/or directly into the streams, lakes of each catchment area, which discharges its water and waterborne solute mass flows into a downstream recipient. This recipient is the coastal water for both catchment areas investigated here, with a single coastal outlet in the Norrström basin, and multiple stream outlets as well as zones of direct groundwater discharge to the coast in the Forsmark catchment area (Fig. 1).

The advective solute travel time from any mass input location a_{gw} along the mean groundwater flow direction x_{gw} to a given control plane location x_{CP} along that direction (e.g., at the nearest groundwater–stream or groundwater–coast interface), and a_s along the mean stream/surface water flow direction x_s to the outlet x_{out} is quantified as $\tau_{gw} = \int_{a_{gw}}^{x_{CP}} \frac{dX_{gw}}{v_{gw}(X_{gw})}$ and $\tau_s = \int_{a_s}^{x_{out}} \frac{dX_s}{v_s(X_s)}$, with $v_{gw}(X_{gw})$ and $v_s(X_s)$ being the local transport velocity in the x_{gw} and x_s direction at advective solute transport position X_{gw} and X_s along x_{gw} and x_s, respectively. For any solute input location at the catchment surface, a total flow-weighted average travel time T to the recipient can be quantified as $T = (1-\beta_{gw})\tau_s + \beta_{gw}(\tau_{gw} + \tau_s)$, or just $T = \tau_{gw}$ in near-coastal catchment zones with only groundwater flow to the coast (see Forsmark area in Fig. 1b), where β_{gw} is the flow fraction of the total precipitation surplus (precipitation minus actual evapotranspiration) at the catchment surface that infiltrates the soil–groundwater system, and $(1 - \beta_{gw})$ is the complementary fraction that flows directly into the recipient through only surface runoff and stream flow. In general, $\beta_{gw} = 0$ in all catchment area parts that are covered by surface water, while it may generally have different values at different land surface locations. In the present calculations, explained further in the specific catchment sections below, β_{gw} is assumed steady in time and is estimated mainly from available land cover information for the Forsmark catchment area, and both land cover and river network information for the Norrström drainage basin.

The quantification of delivered solute mass fraction from the catchment surface to the coast is made here for solute that undergoes first-order attenuation $exp(-\lambda_{gw}\tau_{gw})$ in the subsurface and $exp(-\lambda_s\tau_s)$ in the stream network system of the catchment. For simplicity, because we do not investigate any specific tracer, nutrient or pollutant transport situation, we illustrate results for $\lambda_{gw} = \lambda_s = \lambda$, so that the mass delivery fraction α from any input location to the coast is quantified as $\alpha = exp(-\lambda T)$. The total delivered mass fraction from the whole catchment to the coast is quantified by the mean value, $\overline{\alpha}$, of α for uniform mass input over the whole catchment surface.

2.3 The Forsmark and Norrström catchment areas

The Forsmark catchment area is relatively small (30 km^2) and characterized by uniquely high-resolved (on 10 m × 10 m grid cells) measured and modeled hydrological data [25–28]. The Norrström drainage basin is relatively large (22000 km^2), with much coarser (1 km × 1 km) resolution of available measured and modeled data [19–24]. This section shortly describes the main flow and transport characteristics of these areas. More details on the modeling and calculations for each area are given in Appendix.

2.3.1 Forsmark catchment area

The Forsmark catchment area (Fig. 1b) contains the subcatchments (black contours, Fig. 1b) of ten main stream-outlets to the Baltic Sea, with small near-coastal catchment zones in between discharging mainly groundwater to the sea. The Forsmark catchment area is currently of particular interest due to its consideration by the Swedish Nuclear Fuel and Waste Management Company as a possible suitable location for a deep repository for spent nuclear fuel, e.g., [26,56]. Quaternary deposits cover a major part of the surface and are dominated by till (mainly sandy). The land surface is mainly covered by forest. There are also many lakes and wetlands, with the wetlands being sometimes partially forested. Figure 1b shows the ten main connected stream networks (with outlets to the coast shown with black dots) and their catchments (with boundaries drawn with black lines), where the dominating flow and transport pathways from the land surface to the coastal waters go through the coupled groundwater–stream system to the nearest surface water (stream, lake, wetland) and through the associated stream network to the coast. The remaining surface area in the Forsmark catchment represents the about 11% of the total catchment surface area that is covered by the small, near-coastal catchment zones where groundwater discharges directly into the coastal waters.

In general, infiltration excess overland flow may occur in this catchment area but only over short distances [56,57], implying a negligible surface runoff contribution to the total runoff from the catchment and thereby $\beta_{gw} \approx 1$ in the land surface grid cells, which cover about 85% of the catchment area. The remaining 15% is covered by surface water (streams, lakes and wetlands), for which $\beta_{gw} = 0$.

The fine data and model resolution for this catchment area allows us to investigate the role of the groundwater hydraulic gradient quantification, by using the same underlying fine-resolved (10 m $\times$ 10 m grid) ground slope data as in previously reported hydrological modeling [26,28] in two different ways. Specifically, we estimate the hydraulic gradient in each grid cell in the groundwater system as equal to: either (i) the arithmetic mean value of all the local, fine-resolved ground slopes in the subcatchment area of the outlet (to the nearest stream or directly to the sea) that is associated with the grid cell; this slope is then constant among the different grid cells within each subcatchment area and referred to as the subcatchment-average slope and hydraulic gradient; or (ii) the fine-resolved local ground slope at each grid cell location, which we refer to as the local ground slope and groundwater hydraulic gradient. Grid cell lengths through each model cell are generally for both gradient approaches calculated in the horizontal plane, based on estimated flow path directions and the size of model grid cells. Elevation is thus not accounted for in the transport distance calculations, which implies that any result differences between the different gradient estimation approaches depend on associated transport velocity and not transport length differences.

Field measurements of hydraulic conductivity (by 36 slug tests and 2 pumping tests) throughout the Forsmark catchment area yielded highly variable conductivity values, which were generally higher at the interface between the quaternary deposits and the underlying bedrock than in the soil above that interface [57]. For the investigation purposes of the previous hydrological modeling studies of this area [26,28], a uniform hydraulic conductivity value (equal to the reported mean value from measurements [57]) was used to mainly represent the solute transport through the high-conductivity layer at the soil–bedrock interface. The same model representation is used also here, allowing us to investigate the effect of different assumptions with regard to the spatial variability of hydraulic conductivity, by comparison with Norrström basin results under similar mean travel time conditions.

2.3.2 Norrström drainage basin

The Norrström drainage basin (Fig. 1c) is defined by the coastal outlet location of Norrström in the Swedish capital, Stockholm, and contains many (sixty shown in Fig. 1c) main subcatchments that drain their water through the major lake Mälaren to that common outlet and further into the Baltic Sea. The basin is rather flat with a basin-average topographic slope of 1.5% and a steepest topographic slope of 10% in a single 1 km × 1 km model grid cell, and low-lying with numerous lakes, underlain by granitic and gneiss-granitic bedrock covered by clay or till deposits. On the resolution scale of 1 km × 1 km, land-cover is classified to consist of 4% built-up areas, 36% agricultural and open land, 49% forest, 1.5% wetlands and 9.5% major inland surface waters.

Due to the coarse spatial model resolution of this basin, there are generally unresolved streams and other surface water features also within the model grid cells that are classified as land. Given a relevant stream density for these grid cells based on several paper and digital sources for river network delineation [19], the previous hydrological model studies of the Norrström basin [19–24] have quantified the total flow from the land–soil–groundwater system that feeds the surface water system to be, on average, about 75% of the total water flow through the basin. The remaining flow of about 25% goes then only through the surface water system. In these surface water cells defined by land cover and river network information, $\beta_{gw} = 0$. In the land–soil–groundwater system grid cells, $\beta_{gw} = 1$ because the pure surface runoff contribution to the total (surface and land–soil–ground) water flow is negligible (about 0.02%) in Norrström, as in Forsmark.

The previous, underlying hydrological modeling of the Norrström basin [21] conceptualized the groundwater flow to be partitioned between a relatively highly conductive (shallow, e.g., of quaternary deposits) and a less conductive (deeper, e.g., the bedrock) groundwater subsystem with the average total thickness of the two groundwater systems being set to 50 m following de Wit [58]. In this study, we investigate specifically the advective travel time effects of accounting for or neglecting the possible flow partitioning into the groundwater subsystem of slower/deeper flow.

Due to the coarse spatial resolution, the grid cell-average hydraulic gradient quantification for the groundwater system in the Norrström basin is more consistent with the subcatchment-average than with the local gradient estimate in the Forsmark catchment area. In contrast to the Forsmark application, the groundwater hydraulic conductivity in Norrström is modeled to vary between grid cells, depending on the available data of soil characteristics [19–24].

3 Results and discussion

Figure 2 illustrates the spatial and statistical distributions of advective travel times through the different water subsystems, and in total through the catchment area to the coast, from all the 10 m × 10 m grid cells in Forsmark, with the different hydraulic gradient quantifications: (i) the subcatchment-average gradient (Fig. 2a, b), and (ii) the local gradient (Fig. 2c, d). The different gradient quantifications yield large travel time differences in both the spatial distribution (Fig. 2a, c) and the spreading of the statistical distribution (Fig. 2b, d) of travel times. The differences depend on the contributions of very long travel time components in the local gradient approach from the large flat-topography parts of the Forsmark area. The arithmetic averaging involved in the subcatchment-average gradient approach reduces the weight of small local gradient values and provides more realistic estimates of the prevailing hydraulic gradient, which is not likely to fluctuate as much as the local ground slope.

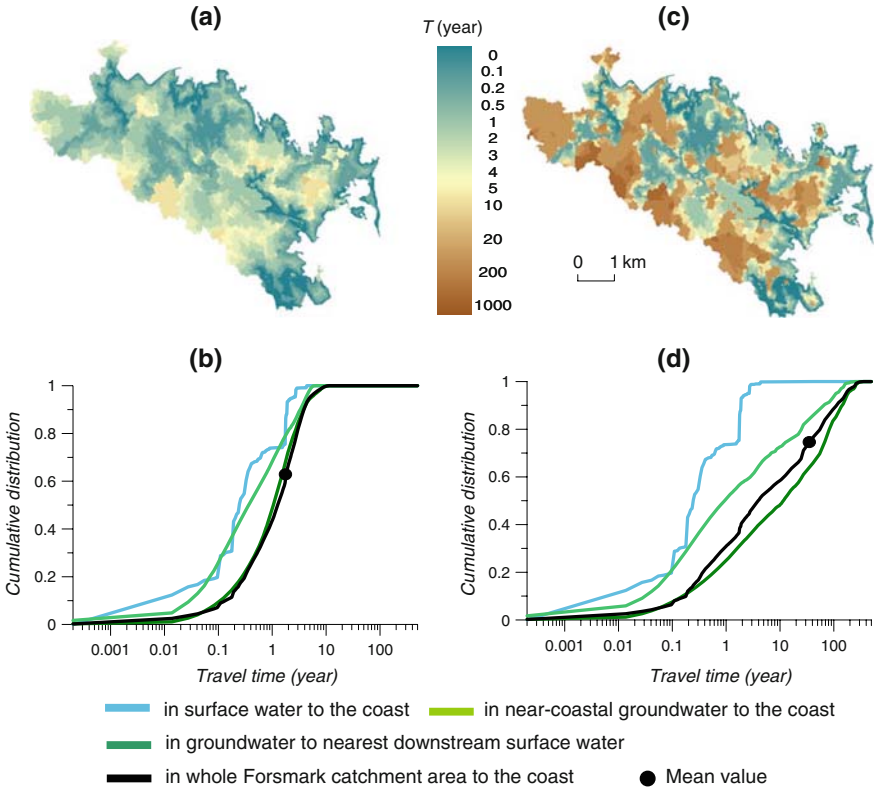

Fig. 2 Spatial (**a**, **c**) and statistical (**b**, **d**) distributions of advective travel time from all grid cells in Forsmark catchment area to the coast, for the stream network and groundwater subsystems and the whole catchment, with hydraulic gradient quantification from **a**, **b** subcatchment-average ground slope; and **c**, **d** local ground slope

The differences in Fig. 2 underline the essential role of the model representation of groundwater hydraulics, here reflected by the different possible approaches to estimate the hydraulic gradient. The fact that infiltration excess overland flow is negligible in Forsmark [56,57] explains the strong hydraulic gradient control on calculated advective travel times through this catchment area, which was also found by McGuire et al. [15]. A contrasting and counter-intuitive positive relationship between catchment transit times and ground slope has been found by Tetzlaff et al. [59] for the flat Swedish Krycklån boreal basin. This result is explained by the total runoff being dominated by relatively fast overland flow, rather than by groundwater flow as in Forsmark, in the flatter, poorly drained peat soils of the Krycklån basin [60].

Figure 3 illustrates the spatial and statistical distributions of advective travel times through the different water subsystems and the whole basin to the coast from all the 1 km × 1 km grid cells in Norrström. Results are illustrated for the alternative model representations that neglect (Fig. 3a, b) or account for (Fig. 3c, d) the possible contribution of slow/deep groundwater flow. The travel time differences obtained by these alternative model representations are large in terms of both the spatial distribution (Fig. 3a, c) and the statistical spreading (Fig. 3b, d) of travel times in the basin. Since flow path directions and flow pathway lengths are the same in

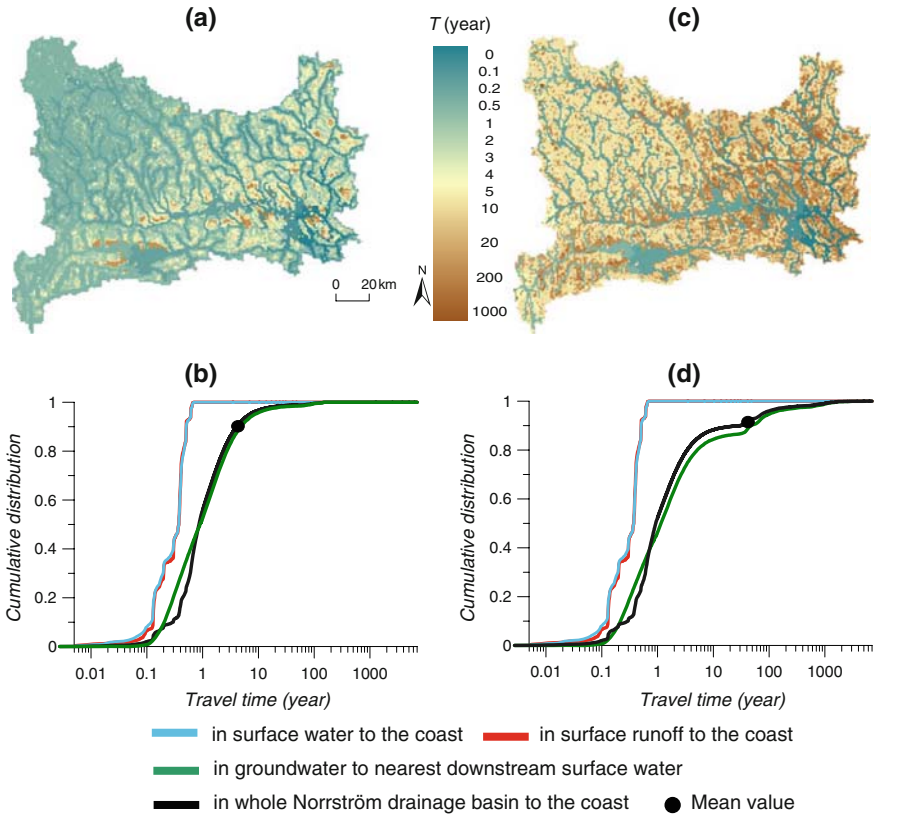

Fig. 3 Spatial (**a**, **c**) and statistical (**b**, **d**) distributions of advective travel time from all grid cells in the Norrström drainage basin to the coast, for the surface runoff, surface water and groundwater subsystems and the whole catchment for **a**, **b** neglect and **c**, **d** account for the possible contribution of a slow/deep groundwater subsystem

both conceptualizations, these travel time distribution differences are only due to the assumed partitioning (in Fig. 3c, d) or the no-partitioning (in Fig. 3a, b) of groundwater flow between the two groundwater subsystems with distinctly different advective velocities. Also these differences emphasize thus the importance of relevant groundwater system characterization for relevant and accurate assessment of solute travel time distributions in catchments.

The importance of groundwater controls on catchment-scale travel times has also been reported in other studies, which have found greater travel time dependence on bedrock seepage [61,62] than on the more directly intuitive catchment size. The results illustrated in Fig. 3 show that also in the Norrström basin, the relatively small proportion of about 12% of the total runoff recharging the slow/deep groundwater subsystem is sufficient for significantly increasing the total mean travel time to the coast. With this deep recharge fraction, the mean total travel time increases from about 3 to about 30 years (Fig. 3). Furthermore, the travel time variability, quantified in terms of the travel time standard deviation, increases from about 10 to about 60 years (Fig. 3).

Table 1 summarizes the most directly comparable catchment-scale travel time statistics for the two catchment areas: those for the case of neglecting the slow/deep groundwater

Table 1 Catchment-scale mean value, standard deviation and coefficient of variation of advective travel times T from all grid cells in the Forsmark and Norrström catchment areas to the coast

Advective travel time to the coast in the Forsmark catchment area		Advective travel time to the coast in the Norrström drainage basin	
Mean value (years)	1.7	Mean value (years)	3.4
Standard deviation (years)	1.7	Standard deviation (years)	11.2
Coefficient of variation	1.0	Coefficient of variation	3.3

Travel times in Forsmark are for the subcatchment-average hydraulic gradient quantification. Travel times in Norrström neglect the possible contribution of slow/deep groundwater

flow contribution in Norrström (Fig. 3a, b), and the case of subcatchment-average hydraulic gradient in Forsmark (Fig. 2a, b). Under these conditions, the resulting total mean travel time is similar for both catchment areas. To explain this similarity, Tables 2 and 3 in Appendix summarize some characteristic flow and transport parameter statistics for these Forsmark and Norrström cases, respectively. A comparison between these tables shows that, beyond the similar precipitation surplus because both catchments are in the same hydro-climatic region, the similarity in mean advective travel times between the two cases depends on their similar mean combined times for advective groundwater transport, expressed as the mean value of the ratio between groundwater flow path length and groundwater flow velocity (in turn quantified as the product of hydraulic conductivity and slope divided by porosity). This time scale is similar even though the separate groundwater flow and transport characteristics are quite different between the two cases, and irrespectively of the very different catchment area sizes. The independence of mean travel time on catchment scale is consistent with similar findings for diffuse solute transport by McGuire et al. [15], Tetzlaff et al. [59] and Rodgers et al. [63], however depending on different types of flow and transport controls in the different catchment case studies.

The main groundwater system control of the Forsmark and Norrström travel time results is emphasized by the order-of-magnitude smaller standard deviation and the three times smaller coefficient of variation of advective travel times (from different input positions to the coast) in Forsmark than in Norrström (Table 1). Specifically, comparison between Tables 2 and 3 with regard to the coefficients of variation of different flow and transport parameters shows that the uniform hydraulic conductivity and porosity assumption for the groundwater system in Forsmark is primarily responsible for its small travel time variability (in terms of both standard deviation and coefficient of variation). This variability difference implies a much greater spatio-temporal spreading (macro-dispersion) of solute around its centre of mass in Norrström than in Forsmark, and emphasizes the importance of spatial groundwater variability assumptions for the distributions of advective solute travel time and the associated physical spreading of solute mass in catchment-scale hydrological transport.

Figure 4 finally illustrates the effect of these variability differences for the delivered solute mass fraction from different input locations to the coast in the comparable (in terms of similar mean travel time) Norrström (Fig. 4a–c) and Forsmark (Fig. 4d–f) cases, for different scenarios of the product of catchment-average physical travel time $\check{T}$ and biogeochemical attenuation rate λ. For each catchment area and $\lambda\check{T}$ scenario, Fig. 4 shows also the total resulting catchment-scale delivery fraction $\overline{\alpha}$ of solute mass to the coast.

The results in Fig. 4 indicate that the differences in solute travel time variability implied by the different spatial variability assumptions for the groundwater hydraulic parameters in the two catchment case quantifications are primarily important in solute-catchment situations where $0.1 < \lambda\check{T} < 10$. For the interval $0.1 < \lambda\check{T} < 10$, any uniform, instantaneous solute mass

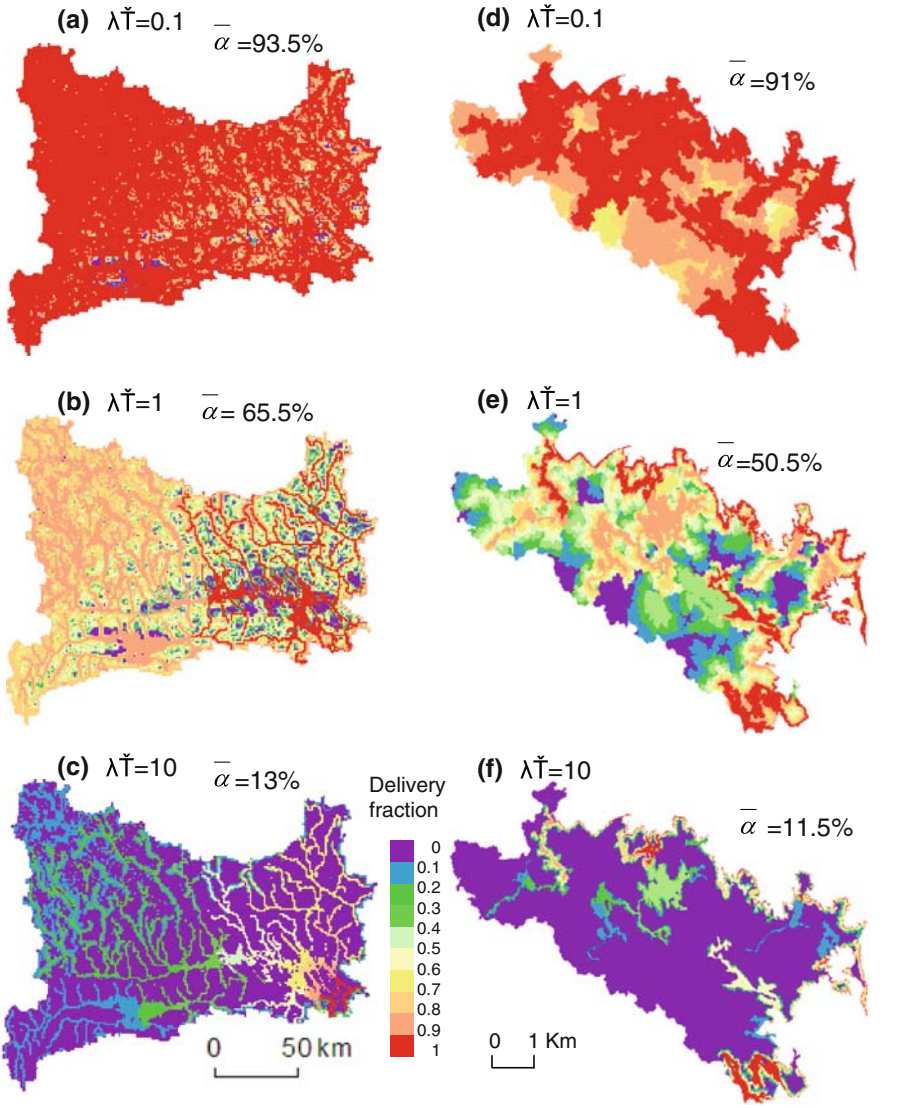

Fig. 4 Map of delivered mass fraction from each grid cell location to the coast in the Norrström drainage basin (**a**–**c**) and Forsmark catchment area (**d**–**f**), for different scenarios (0.1, 1 and 10) of the product of catchment-average advective travel time $\check{T}$ and attenuation rate λ. The total delivered mass fraction $\bar{\alpha}$ from the whole catchment area is also quantified in the figure for each $\lambda\check{T}$ scenario. Travel times in Norrström (**a**–**c**) neglect the possible contribution of slow/deep groundwater. Travel times in Forsmark (**d**–**f**) are for the subcatchment-average hydraulic gradient

input leads to a delivered mass fraction that is about 30% (or 15 percentage units) greater for the Norrström case with the larger advective travel time variability than for the Forsmark case with the smaller travel time variability. Smaller or greater mean $\lambda\check{T}$ scenarios than this $0.1 < \lambda\check{T} < 10$ interval imply nearly non-attenuated or nearly totally attenuated solute mass, respectively, essentially regardless of the prevailing variability of advective solute travel times.

4 Conclusion

This study has outlined the possible quantification of advective solute travel-time distributions in different catchment areas. The specific catchment cases in the study differ largely in terms of their scale, data-model resolutions, and process representations in the travel time modeling. Yet the comparative analysis of these cases has provided some important general insights.

The results show that the groundwater system characterization and model representation largely controls the resulting distributions of advective travel times through these hydrological catchments. For groundwater assumptions that yielded similar catchment-average travel times in the different catchment cases, the spatial variability in groundwater hydraulics played an essential role for the travel time variance, which determines the physical spreading (macrodispersion) of non-reactive solute mass transported through the catchment.

For solute that is physically or biogeochemically attenuated along its different transport pathways through the catchment, the product of the catchment-average advective travel time and the solute-dependent biogeochemical attenuation rate was shown to largely determine the effects of travel time variance on the total solute mass delivery from the catchments. These effects were found to be primarily important for the product interval $0.1 < \lambda\check{T} < 10$. For hazardous contaminants, where even very small solute concentrations and concentration differences may be essential for environmental and health risks, however, the travel time variability effects may be important and need to be further investigated also for $\lambda\check{T} \geq 10$.

Furthermore, the primary importance-interval $0.1 < \lambda\check{T} < 10$ applies to the investigated conditions of variability only in the physical, advective travel time T. The interval may widen significantly if also the attenuation rate λ is variable, and depending on its possible cross-correlation with the advective travel time T [e.g., 34,64–66]. Further investigations and realistic quantifications are needed for the spatial variability of biogeochemical attenuation rates and their correlation with the physics of flow and transport in both the surface water and not least the groundwater systems of hydrological catchments.

Acknowledgements Financial support for this work has been provided by the Swedish Research Council (VR), the Swedish Rescue Services Agency (Räddningsverket), and the Swedish Nuclear Fuel and Waste Management Company (SKB).

Appendix

Modeling of the Forsmark catchment area

The previous hydrological modeling of the Forsmark catchment area [25–28], described in detail by Jarsjö et al. [25,26,28], provides the spatial distribution of total (surface and subsurface) annual average runoff (over 30 years), as estimated from the modeled precipitation surplus, which is the difference between annual average precipitation and modeled actual evapotranspiration in each model cell. The direction of the water flow and solute transport pathway through each cell of the modeled catchment area is estimated from the local ground slope, which is in turn estimated from a detailed digital elevation model of the area, as explained in more detail by Jarsjö et al. [25,26,28]. The present Forsmark application is based on average results from two different empirical approaches [67,68], which were used for actual evapotranspiration calculations in the previous, underlying hydrological modeling and yielded consistent resulting spatial water flow distribution with each other and consistent water flow results with independent runoff data from the catchment area.

To obtain the travel time from each input cell a_{gw} along the associated groundwater pathway (as estimated from the ground slope direction) to the control plane at distance x_{cp} (of the nearest stream and/or the coast), the travel time contribution $\Delta\tau_{gw} = \Delta x_{gw}/v_{gw}$ of each model cell is estimated from the cell length Δx_{gw} and the transport velocity $v_{gw} = K \cdot I/n$, where K is hydraulic conductivity, I is hydraulic gradient, and n is effective porosity. The total mean $\tau_{gw}(a_{gw}, x_{CP})$ is the sum of $\Delta\tau_{gw}$ for all cells along the transport pathway to x_{cp}. The hydraulic conductivity and effective porosity are assumed to be $1.5 \cdot 10^{-5}$ m/s and 0.05, respectively, over the whole catchment area, as reported by Johansson et al. [57] for the quaternary deposits/bedrock interface. In the subcatchment-average gradient approach (i) in the main text, the hydraulic gradient in each grid cell is set equal to the arithmetic average of all the local ground slopes in the subcatchment area of the associated grid-cell outlet to the nearest stream or directly to the sea. The hydraulic gradient is then constant among the different grid-cells within each subcatchment area, including in cells with nearly zero local ground slope. In the local gradient approach (ii) in main text, the local hydraulic gradient in each cell equals the local ground slope in that cell.

The stream network includes all the interconnected bodies of surface water, streams, lakes and wetlands, through which the waterborne solute mass may be transported all the way to the coast. For obtaining the travel time from each input cell a_s along the associated stream network pathway to the outlet at x_{out}, the travel time contribution $\Delta\tau_s = L_s/v_s$ of each stream stretch is estimated from its length Ls and mean flow velocity $v_s = Q/A_{cs}$, where Q is the mean annual flow rate and A_{cs} is the mean cross-sectional area of the stream. The total mean $\tau_s(a_s, x_{out})$ is the sum of $\Delta\tau_s$ for all the stream stretches, lakes and wetlands along the whole stream network pathway to x_{out}; the estimation of $\Delta\tau_s$ in lakes and wetlands is explained below. In streams where the mean cross-sectional area is measured and known (from 0.29 to 0.43 m^2), Q is assumed to be equal to the modeled mean annual water flow at the model cell location where the stream cross-section area was measured. Otherwise, a generic value of $A_{cs} = 0.3\,m^2$ and the modeled [25,26,28] mean annual flow value at the mouth of the stream are used in the calculation of mean flow velocity. The $\Delta\tau_s$ contribution of a lake or a wetland is estimated as $\Delta\tau_s = A_{L/W} \cdot d_{eff}/Q$, where $A_{L/W}$ is the area of the lake or wetland, Q is the mean annual flow rate through the lake or wetland, and d_{eff} is the mean depth in lakes and is defined as the product of the depth and the water content (typically around 0.9) in wetlands. The mean flow rate Q is the modeled [25,26,28] mean annual runoff (precipitation minus evaporation) generated in the lake or wetland plus the modeled [25,26,28] runoff into the lake or wetland from all upstream cells. For isolated lakes and wetlands that are not part of any connected stream network pathway all the way to the coast, their travel time contribution is calculated from the length of a topographically estimated transport pathway through the lake or wetland divided by an average velocity $v_{L/W} = Q\sqrt{[4A_{L/W}/\pi]}/[A_{L/W} \cdot d_{eff}]$, where $\sqrt{[4A_{L/W}/\pi]}$ is the diameter of a circle with the same area $A_{L/W}$ as the lake or wetland. The travel time contribution obtained is added to the total groundwater travel time τ_{gw} along the main groundwater pathway that crosses the isolated lake or wetland. Details on measured lake and wetland depths are given by Johansson [69] and Brunberg et al. [70].

Modeling of the Norrström drainage basin

The previous hydrological modeling of the Norrström drainage basin [19–24], described in detail by Darracq et al. [21] after de Wit [58,71] and Greffe [72], provides the spatial distribution of total (surface and subsurface) annual average runoff (over 30 years),

as estimated from the modeled precipitation surplus in each model cell; as in Forsmark, the precipitation surplus is also here defined as the difference between annual average precipitation and actual evapotranspiration, modeled based on an empirical function of precipitation and potential evapotranspiration [67,73]. A digital elevation map available at a resolution of 1 km × 1 km was used for assigning water flow and solute-transport pathway directions through each cell of the modeled catchment area. Previous hydrological modeling results in the Norrström basin [21] are also used to obtain: the contribution of the flow through the land–soil–groundwater system to the total water flow through the basin, based on the ratio between the long-term average groundwater recharge and the total precipitation surplus in each grid cell, as functions of land cover and topographic slope [68]; and the travel time $\tau_{gw}(a_{gw}, x_{CP})$ from each grid cell a_{gw} along the groundwater pathway (as estimated from the ground slope direction) to the control plane at distance x_{cp} of the nearest stream.

As mentioned also in the main text, the previous hydrological modeling of the Norrström basin [21] conceptualized the groundwater flow to be partitioned between a relatively highly conductive (shallow, e.g., of quaternary deposits) and a less conductive (deeper, e.g., the bedrock) groundwater subsystem, with the groundwater flow depending on aquifer type, soil texture, groundwater level, slope, land use and average January temperature [73] based on empirical estimates by de Wit [58] and Mourad [74]. Following Wendland [68], the travel time $\tau_{sgw}(a_{gw}, x_{CP})$ from each input cell a_{gw} along the associated pathway (as estimated from the ground slope direction) in the fast/shallow groundwater subsystem to the nearest stream at x_{cp} is quantified as: $\tau_{sgw} = lp/v$, where v is the groundwater flow velocity and lp is the average length of the groundwater flow path, as a function of conductivity of the aquifer ca, hydraulic gradient h(with topographic slope in each 1000 m grid cell used as an estimate of h), primary effective aquifer porosity pp and modeled total runoff Q. Specifically, $v = ca \cdot h/pp$ and $lp = 0.5/ns$, where ns is stream density quantified as $ns = 2$ in wetlands and $(Q/450)^{0.8}$ (with Q given in mm year^{-1}) elsewhere.

Furthermore, following Meinardi et al. [73], the travel time $\tau_{dgw}(a_{gw}, x_{CP})$ from each grid cell a_{gw} along the pathway in the slow/deep groundwater subsystem to the nearest stream at x_{cp} (the transport length of which is estimated similarly as in the fast/shallow groundwater system, from the ground slope direction) is calculated as the product between total effective porosity of the aquifer tp, thickness of groundwater flow formation at and the inverse of the long-term average recharge of the slow/deep groundwater subsystem. The average total thickness of both groundwater systems over the whole Norrström basin is set to 50 m following de Wit [58]. Values for aquifer conductivity, primary and total porosity are empirically related [58,68,73] to the aquifer type and the soil and bedrock groundwater flow yields, which were obtained for the Norrström basin from the Swedish Geological Survey mapping of groundwater in soil and bedrock.

The resulting total groundwater travel time $\tau_{gw}(a_{gw}, x_{CP})$ is quantified as: $\tau_{gw} = (1 - \beta_{dgw}) \cdot \tau_{sgw} + \beta_{dgw} \cdot \tau_{dgw}$, where β_{dgw} is the recharge of the slow/deep groundwater subsystem, in terms of flow fraction of the total groundwater flow into the surface water system; that fraction was on average about 12% of the total flow in the previous model simulations [19–24], implying that $\beta_{dgw} = 0.12$ in the present results that account for the possible slow/deep groundwater flow contribution, and $\beta_{dgw} = 0$ in the results that neglect it (Tables 2, 3).

The stream network includes all the interconnected bodies of surface water, streams and lakes through which the waterborne mass may be transported all the way to the coast. For obtaining the travel time from each cell a_s along a stream network pathway to the outlet at x_{out}, the travel time contribution $\Delta\tau_s = L_s/v_s$ of each stream stretch is estimated from

Table 2 Mean value, standard deviation and coefficient of variation of precipitation surplus (i.e., precipitation minus actual evapotranspiration), topographic slope, groundwater system porosity, hydraulic conductivity and flow path length, and the combined characteristic time for groundwater transport expressed by the fraction: $\frac{\text{groundwater\_flow\_path\_length}}{\frac{\text{conductivity}^{*}\text{slope}}{\text{porosity}}}$ in the Forsmark catchment area

	Mean value	Standard deviation	Coefficient of variation
Precipitation surplus (mm/year)	226	35	0.2
Slope	0.03	0.01	0.3
Porosity	0.05	0	0
Hydraulic conductivity (m/day)	1.3	0	0
Groundwater flow path length (m)	394	491	1.2
$\frac{\text{groundwater\_flow\_path\_length}}{\frac{\text{conductivity}^{*}\text{slope}}{\text{porosity}}}$ (years)	1.5	1.8	1.2

Table 3 Mean value, standard deviation and coefficient of variation of precipitation surplus (i.e., precipitation minus actual evapotranspiration), topographic slope, groundwater system porosity, hydraulic conductivity and flow path length, and the combined characteristic time for groundwater transport expressed by the fraction: $\frac{\text{groundwater\_flow\_path\_length}}{\frac{\text{conductivity}^{*}\text{slope}}{\text{porosity}}}$ in the Norrström drainage basin

	Mean value	Standard deviation	Coefficient of variation
Precipitation surplus (mm/year)	233	50	0.2
Slope	0.01	0.01	1.0
Porosity	0.18	0.3	1.6
Hydraulic conductivity (m/day)	125	295	2.4
Groundwater flow path length (m)	1042	299	0.3
$\frac{\text{groundwater\_flow\_path\_length}}{\frac{\text{conductivity}^{*}\text{slope}}{\text{porosity}}}$ (years)	3.4	12	3.6

its length L_s and mean flow velocity v_s, empirically estimated from an expression given in [20,75], as: $v_s = 0.36Q^{0.241}$ in streams and $v_s = 0.36(Q/A_L)^{0.241}$ in lakes, where Q is mean annual flow rate in m^3/s as obtained from previous hydrological modeling [21] and A_L is lake surface area. The total τ_s (a_s, x_{out}) is the sum of $\Delta\tau_s$ for all the stream stretches and lakes along the whole stream network pathway and topographically estimated transport pathway through lakes to x_{out}.

The travel time contributions $\Delta\tau_{sr=}L_{sr}/v_{sr}$ in the surface runoff subsystem is estimated in analogy with the stream network subsystem, from the surface runoff pathway length L_{sr} and mean flow velocity $v_s = 0.36(Q)^{0.241}$, where Q is modeled surface runoff flow in m^3/s. In the combined total travel time distribution through the whole basin, the weight of the surface runoff contribution is negligible (0.02%) compared to the groundwater flow, so that results are directly comparable between Norrström and Forsmark.

References

1. McGuire KJ, McDonnell JJ (2006) A review and evaluation of catchment transit time modeling. J Hydrol 330:543–563
2. Maloszewski P, Zuber A (1982) Determining the turnover time of groundwater systems with the aid of environmental tracers. 1. Models and their applicability. J Hydrol 57:207–231
3. Simic E, Destouni G (1999) Water and solute residence times in a catchment: stochastic model interpretation of 18O transport. Water Resour Res 35(7):2109–2120
4. Lindgren GA, Destouni G (2004) Nitrogen loss rates in streams: scale-dependence and up-scaling methodology. Geophys Res Lett. doi:10.1029/2004GL019996
5. Lindgren GA, Destouni G, Miller AV (2004) Solute transport through the integrated groundwater–stream system of a catchment. Water Resour Res. doi:10.1029/2003WR002765
6. Botter G, Bertuzzo E, Bellin A, Rinaldo A (2005) On the Lagrangian formulations of reactive solute transport in the hydrologic response. Water Resour Res. doi:10.1029/2004WR003544
7. Fiori A, Russo D (2008) Travel time distribution in a hillslope: insight from numerical simulations. Water Resour Res. doi:10.1029/2008WR007135
8. Schnoor JL (1996) Environmental modeling: fate and transport of pollutants in water, air and soil. Wiley, New York
9. Rinaldo A, Marani A, Rigon R (1991) Geomorphological dispersion. Water Resour Res 27(4):513–525
10. White AB, Kumar P, Saco PM, Rhoads BL, Yen BC (2004) Hydrodynamic and geomorphologic dispersion: scale effects in the Illinois River Basin. J Hydrol 288:237–257
11. Saco PM, Kumar P (2002) Kinematic dispersion in stream networks 1. Coupling hydraulic and network geometry. Water Resour Res. doi:10.1029/2001WR000695
12. Valett HM, Morrice JA, Dahm CN, Campana ME (1996) Parent lithology, surface-groundwater exchange, and nitrate retention in headwater streams. Limnol Oceanogr 41(2):333–345
13. Ensign SH, Doyle MW (2005) In-channel transient storage and associated nutrient retention: evidence from experimental manipulations. Limnol Oceanogr 50(6):1740–1751
14. Haggerty R, Wondzell SM, Johnson MA (2002) Power-law residence time distribution in the hyporheic zone of a 2nd-order mountain stream. Geophys Res Lett. doi:10.1029/2002GL014743
15. McGuire KJ, McDonnell JJ, Weiler M, Kendall C, McGlynn BL, Welker JM, Seibert J (2005) The role of topography on catchment-scale water residence time. Water Resour Res 41(5):W05002.1–W05002.14
16. Boano F, Packman AI, Cortis A, Revelli R, Ridolfi L (2007) A continuous time random walk approach to the stream transport of solutes. Water Resour Res. doi:10.1029/2007WR006062
17. Wörman A, Packman AI, Marklund L, Harvey J, Stone S (2007) Fractal topography and subsurface water flows from fluvial bedforms to the continental shield. Geophys Res Lett. doi:10.1029/2007GL029426
18. Malmström ME, Destouni G, Banwart SA, Strömberg BHE (2000) Resolving the scale-dependence of mineral weathering rates. Environ Sci Technol 34:1375–1378
19. Darracq A, Destouni G (2005) In-stream nitrogen attenuation: model-aggregation effects and implications for coastal nitrogen impacts. Environ Sci Technol 39(10):3716–3722
20. Darracq A, Destouni G (2007) Physical versus biogeochemical interpretations of nitrogen and phosphorus attenuation in streams and its dependence on stream characteristics. Glob Biogeochem Cycles. doi:10.1029/2006GB002901
21. Darracq A, Greffe F, Hannerz F, Destouni G, Cvetkovic V (2005) Nutrient transport scenarios in a changing Stockholm and Mälaren valley region. Water Sci Technol 51(3-4):31–38
22. Destouni G, Darracq A (2006) Response to comment on "In-stream nitrogen attenuation: model aggregation effects and implications for coastal nitrogen impacts". Environ Sci Technol 40(7):2487–2488
23. Lindgren GA, Destouni G, Darracq A (2007) The inland subsurface water system role for coastal nitrogen load dynamics and abatement responses. Environ Sci Technol 41(7):2159–2164
24. Darracq A, Lindgren GA, Destouni G (2008) Long-term development of phosphorus and nitrogen loads through the subsurface and surface water systems of drainage basins, Global Biogeochem Cycles. doi:10.1029/2007GB003022
25. Jarsjö J, Shibuo Y, Destouni G (2004) Using the PCRaster-POLFLOW approach to GISbased modelling of coupled groundwater–surface water hydrology in the Forsmark Area. Swedish Nuclear Fuel and Waste Management Company Report R-04-54, Stockholm, Sweden
26. Jarsjö J, Destouni G, Persson K, Prieto C (2007) Solute transport in coupled inland-coastal water systems. General conceptualization and application to Forsmark. Swedish Nuclear Fuel and Waste Management Company Report R-07-65, Stockholm, Sweden
27. Destouni G, Shibuo Y, Jarsjö J (2008) Freshwater flows to the sea: spatial variability, statistics and scale dependence along coastlines. Geophys Res Lett. doi:10.1029/2008GL035064

28. Jarsjö J, Shibuo Y, Destouni G (2008) Spatial distribution of unmonitored inland water discharges to the sea. J Hydrol 348(12):59–72
29. Dagan G (1989) Flow and transport in porous formations. Springer Verlag, Berlin
30. Rubin Y (2003) Applied stochastic hydrogeology. Oxford University Press, New York
31. Simmons CS (1982) A stochastic-convective transport representation of dispersion in one-dimensional porous media. Water Resour Res 18:1193–1214
32. Shapiro AM, Cvetkovic V (1998) Stochastic analysis of solute travel time in heterogeneous porous media. Water Resour Res 24:1711–1718
33. Cvetkovic V, Shapiro AM (1990) Mass arrival of sorptive solute in heterogeneous porous media. Water Resour Res 26:2057–2067
34. Destouni G, Cvetkovic V (1991) Field-scale mass arrival of sorptive solute into the groundwater. Water Resour Res 27:1315–1325
35. Destouni G (1993) Stochastic modeling of solute flux in the unsaturated zone at the field scale. J Hydrol 143:45–61
36. Cvetkovic V, Dagan G (1994) Transport of kinetically sorbing solute by steady random velocity in heterogeneous porous formations. J Fluid Mech 265:189–215
37. Destouni G, Sassner M, Jensen KH (1994) Chloride migration in heterogeneous soil: 2, stochastic modeling. Water Resour Res 30:747–758 (Correction, Water Resour Res 31:1161, 1995)
38. Ginn TR, Simmons CS, Wood BD (1995) Stochastic-convective transport with nonlinear reaction: biodegradation with microbial growth. Water Resour Res 31:2689–2700
39. Simmons CS, Ginn TR, Wood BD (1995) Stochastic-convective transport with nonlinear reaction: mathematical framework. Water Resour Res 31:2675–2688
40. Berglund S, Cvetkovic V (1996) Contaminant displacement in aquifers: coupled effects of flow heterogeneity and nonlinear sorption. Water Resour Res 32:23–32
41. Cvetkovic V, Dagan G (1996) Reactive transport and immiscible flow in geochemical media: 2 applications. Proc R Soc Lond Ser A 452:303–328
42. Eriksson N, Destouni G (1997) Combined effects of dissolution kinetics, secondary mineral precipitation, and preferential flow on copper leaching from mining waste rock. Water Resour Res 33: 471–483
43. Yabusaki SB, Steefel CI, Wood BD (1998) Multidimensional, multicomponent, subsurface reactive transport in nonuniform velocity fields: code verification using an advective reactive streamtube approach. J Contam Hydrol 30(3):299–331
44. Foussereau X, Graham W, Aakpoji A, Destouni G, Rao PSC (2001) Solute transport through a heterogeneous coupled vadose-saturated zone system with temporally random rainfall. Water Resour Res 37(6):1577–1588
45. Tompson AFB, Bruton CJ, Pawloski GA, Smith DK, Bourcier WL, Shumaker DE, Kersting AB, Carle SF, Maxwell RM (2002) On the evaluation of groundwater contamination from underground nuclear tests. Environ Geol 42:235–247
46. Cvetkovic V, Haggerty R (2002) Transport with multiple-rate exchange in disordered media. Phys Rev E. doi:10.1103/PhysRevE.65.051308
47. Malmström ME, Destouni G, Martinet P (2004) Modeling expected solute concentration in randomly heterogeneous flow systems with multicomponent reactions. Environ Sci Technol 38:2673–2679
48. Rinaldo A, Marani A (1987) Basin scale model of solute transport. Water Resour Res 23:2107–2118
49. Destouni G, Graham W (1995) Solute transport through an integrated heterogeneous soil–groundwater system. Water Resour Res 31:1935–1944
50. Botter G, Bertuzzo E, Bellin A, Rinaldo A (2005) On the Lagrangian formulations of reactive solute transport in the hydrologic response. Water Resour Res. doi:10.1029/2004WR003544
51. Dagan G, Fiori A (1997) The influence of pore-scale dispersion on concentration statistical moments in transport through heterogeneous aquifers. Water Resour Res 33(7):1595–1606
52. Fiori A, Dagan G (2000) Concentration fluctuations in aquifer transport: a rigorous first-order solution and applications. J Contam Hydrol 45:139–163
53. Fiori A, Berglund S, Cvetkovic V, Dagan G (2002) A first-order analysis of solute flux statistics in aquifers: the combined effect of pore-scale dispersion, sampling, and linear sorption kinetics. Water Resour Res. doi:10.1029/2001WR000678
54. Janssen GMCM, Cirpka OA, Van der Zee EATM (2006) Stochastic analysis of nonlinear biodegradation in regimes controlled by both chromatographic and dispersive mixing. Water Resour Res. doi:10.1029/2005WR004042
55. Malmström ME, Berglund S, Jarsjö J (2008) Combined effects of spatially variable flow and mineralogy on the attenuation of acid mine drainage in groundwater. Appl Geochem 23(6):1419–1436

56. Lindborg T (2005) Description of surface systems. Preliminary site description Forsmark area—version 12. Swedish Nuclear Fuel and Waste Management Company Report R-05-03, Stockholm, Sweden
57. Johansson P-O, Werner K, Bosson E, Juston J (2005) Description of climate, surface hydrology, and near-surface hydrology. Preliminary site description. Forsmark area—version 1.2. Swedish Nuclear Waste Management Company (SKB) Report R-05-06, Stockholm, Sweden
58. de Wit MJM (1999) Nutrients fluxes in the Rhine and Elbe basins. Dissertation, Royal Dutch Geographical Society, Utrecht, Netherlands
59. Tetzlaff D, Seibert J, McGuire KJ, Laudon H, Burns DA, Dunn SM, Soulsby C (2009) How does landscape structure influence catchment transit time across different geomorphic provinces? Hydrol Process 23:945–953
60. Laudon H, Sjöblom V, Buffam I, Seibert J, Mörth CM (2007) The role of catchment scale and landscape characteristics for runoff generation of boreal streams. J Hydrol 344:198–209
61. Asano Y, Uchida T, Ohte N (2002) Residence times and flow paths of water in steep unchannelled catchments, Tanakami, Japan. J Hydrol 261:173–192
62. Dunn SM, McDonnell JJ, Vaché KB (2007) Factors influencing the residence time of catchment waters: a virtual experiment research. Water Resour Res. doi:10.1029/2006WR005393
63. Rodgers P, Soulsby C, Waldron S (2005) Stable isotope tracers as diagnostic tools in upscaling flow path understanding and residence time estimates in a mountainous mesoscale catchment. Hydrol Process 19:2291–2307
64. Jarsjö J, Bayer-Raich M, Ptak T (2005) Monitoring groundwater contamination and delineating source zones at industrial sites: uncertainty analyses using integral pumping tests. J Contam Hydrol 79:107–134
65. Jarsjö J, Bayer-Raich M (2008) Estimating plume degradation rates in aquifers: effect of propagating measurement and methodological errors. Water Resour Res. doi:10.1029/2006WR005568
66. Cunningham JA, Fadel ZJ (2007) Contaminant degradation in physically and chemically heterogeneous aquifers. J Contam Hydrol 94:293–304
67. Turc L (1954) The water balance of soils. Relation between precipitation, evaporation and flow. Annal Agron 5:491–569
68. Wendland F (1992) Die Nitratbelastung in den Grundwasserlandschaften der 'alten' Bundesländer (BRD), Berichte aus der Okologischen Forschung, Band 8, Forschungszentrum Jülich, Jülich
69. Johansson P-O (2003) Drilling and sampling in soil. Installation of groundwater monitoring wells and surface water level gauges. Swedish Nuclear Fuel and Waste Management Company Report P-03-64, Stockholm, Sweden
70. Brunberg A-K, Carlsson T, Blomqvist P, Brydsten L, Strömgren M (2004) Identification of catchments, lake-related drainage parameters and lake habitats. Swedish Nuclear Fuel and Waste Management Company Report P-04-25, Stockholm, Sweden
71. de Wit MJM (2001) Nutrients fluxes at the river basin scale I: the PolFlow model. Hydrol Process 15: 743–759
72. Greffe F (2003) Material transport in the Norrström drainage basin: integrating GIS and hydrological process modelling. Master Thesis, Royal Institute of Technology, Stockholm, Sweden
73. Meinardi C, Beusen A, Bollen M, Klepper O (1994) Vulnerability to diffuse pollution of European soils and groundwater. National Institute of Public Health and Environmental Protection (RIVM), Report 4615001002, Bilthoven, Netherlands
74. Mourad DSJ (2002) Application of GIS-based modelling to assess nutrient loads in rivers of the Estonian part of the lake Peipsi basin. MANTRA-East working paper 5.1
75. Alexander RB, Elliott AH, Shankar U, McBride GB (2002) Estimating the sources and transport of nutrients in the Waikato River Basin, New Zealand. Water Resour Res 38:1268–1290